Journal of Intelligent & Robotic Systems (2019) 95:675–690
https://doi.org/10.1007/s10846-018-0954-x

UAV Traffic Patrolling via Road Detection and Tracking in Anonymous Aerial Video Frames

Mücahit Karaduman[1] · Ahmet Çınar[2] · Haluk Eren[3]

Received: 10 December 2017 / Accepted: 30 October 2018 / Published online: 2 January 2019

Abstract

Unmanned Aerial Vehicles (UAV) have gained great importance for patrolling, exploration, and surveillance. In this study, we have estimated a route UAV to follow, using aerial road images. In the experimental setup, for estimation, test, and validation stages, anonymous aerial road videos have been exploited, meaning a special image database was not produced for this simulation approach. In the proposed study, road portion is initially detected. Two methods are utilized to help road detection, which are k-Nearest Neighbor and Hough transformation. To form a decision loop, both results are matched. If they match each other, they are fused using spatial and spectral schemes for the comparison purpose. Once road area is detected, the road type classification is realized by Fuzzy approach. The resultant image is utilized to estimate route, over which the UAV have to fly towards that direction. In the simulation stage, an anonymous video stream previously captured by UAV is experimented to assess the performance of the underlying system for different roads. According to the implementation results, the proposed algorithm has succeeded in finding all the trial roads in the given aerial images, and the proportion of all the estimated road-portion to actual road pixels for all the images is averagely calculated as %95.40. Eventually, it is shown that UAV has followed the correct route, which is estimated by proposed approach, over the specified road using assigned video frames, and also performances of spatial and spectral fusion results are compared.

Keywords UAV reconnaissance · Nextgen traffic patrolling · Aerial road tracking · Fuzzy classifier · Spatial-spectral fusion · Route estimation

1 Introduction

Today, unmanned aerial vehicles are benefited in many areas covering the military and civil applications. Such vehicles may have advanced imaging systems, and they can be operated by autonomous or remote control. The autonomous UAVs don't need human labor decreasing operational costs. Thus, autonomous operation takes place in numerous applications.

1.1 Motivation

UAVs are getting occupy more place in human life. US Federal Aviation Administration (FAA) defined UAVs with a law as a system flying without a pilot. In this law, different names were given to these types of vehicles, which were UAV, Drone, ECP, and ROA [1].

We can mention about many civil applications of UAVs in the world. For example, Amazon would like to use UAVs for package delivery services, while a Chinese company Ehang introduces a UAV prototype to be able to carry single person [2, 45]. On the other hand, UAVs can be appointed for patrolling several miles-road, which have to fly along a designated route while moving towards a destination. Success of an error-free mission depends on the correct road detection and route planning. Such aerial surveillance systems may take place in different tracking missions including reconnaissance and patrolling. If a UAV is directed to an incorrect route, it may lead to a security flaws and faulty work causing safety-critical issues.

Electronic supplementary material The online version of this article (https://doi.org/10.1007/s10846-018-0954-x) contains supplementary material, which is available to authorized users.

✉ Haluk Eren
he.edu.tr@gmail.com

Extended author information available on the last page of the article.

1.2 Problem Statement

UAVs are assigned to achieve a mission sometimes manually governed by a ground station or semi/full automatically by a software developed. In the road patrolling problem to reach a destination, UAVs have to correctly follow a route as flying over a specified road portion. To accomplish this mission, UAV should initially detect the road, and fly towards estimated direction. Otherwise, UAV may lose the road if it comes across a bend. UAV have to take account for subsequent considerations properly to get the destination:

- UAV camera has to capture successive frames as flying over the road.
- The images should be eliminated from noise.
- The road portion in UAV field of view should be detected.
- Use of validation is suggested to make sure if estimated road is correct.
- Once the validation step is accomplished, spatial and spectral fusion schemes could be processed and compared.
- Road type should be classified.
- The system should allow a proper timing to estimate new direction angle before the drone reaches to next sub-destination.
- The system should be tested by using anonymous videos including different situations and road types such as heavy traffic, curved, or straight road.
- Finally, the route suggestion should be obtained by considering simulated results.

1.3 Proposed Approach

In the first step, UAV should take aerial pictures along the focused road field captured by mounted-camera. In the present study, anonymous videos are employed for a defined task. Considering the flight speed of the UAV, the time-period between two successive pictures are estimated. Therefore, redundant calculations causing time wasting are avoided.

We need to keep in mind that assigned images are not the real images at world coordinate system, but they are images at image plane. Hence, projective geometry plays a significant role in the present scheme. Further, anonymous UAV images may be distorted due to possible vibrations in motion. In such situations, captured images are enhanced by proper noise filters. After reducing noises, we can try to eliminate shadows from the road images using minimum entropy method [3]. Then, present images are converted to binary ones via thresholding. At this point, the road field can be detected by k-Nearest Neighbor (KNN). In order to make sure if the estimated road is the focused road, Hough Transformation (HT) algorithm is simultaneously run. This second round enables first round to be validated. Intersectional segments of road images detected by KNN and HT are extracted for processing, and the rest portions of the images are discarded. As a result of this approach, segmented portion obtained from both results represents the road to be tracked. Until both rounds match each other, the process loops back taking new road images. After that, resultant road type is classified by Fuzzy approach.

As a result of aforementioned stages, two-dimensional route vector values UAV to follow are estimated, each of which addresses a point accommodating abscissa and ordinate components on Cartesian coordinate system. Thus, a temporary route is determined until the subsequent image is captured and processed by UAV. The owner may meet to substantial costs when UAV is lost, but the proposed system avoids UAV of losing its direction under unforeseen conditions that the subject image cannot be appeared temporarily. Energy saving and reduced estimation cost are achieved due to running no extra process in the UAV return cycle.

1.4 Related Work

Researchers associated with road detection or tracking have conducted many studies, in which different methods were employed such as color tones, road marking, and road segments. While some studies take images from ground vehicles [4–7, 9, 10, 12–21], others take images from air vehicles [8, 11, 24–35]. He et al. developed an algorithm detecting road marks and its area. They found road marks from the gray level image, and detected the road field from full color image [4]. Wang et al. used B-spline curve for line detection of curved roads. Both side borders and mid line of the roads were detected by B-spline using the conventional perspective lines [5]. Broggi benefited from a morphological transformation finding lines of subject roads via the perspective projection scheme [6]. Kong et al. generated vanishing point, and then conducted segmentation for detecting candidates of road edges [7]. Lin et al. used histogram based adaptive thresholding algorithm for detection of possible roads. Then, they found road line by probabilistic Hough transformation [8]. Fernandez et al. classified the colors on the road, and then the detection process was realized by a decision tree [9]. Alvarez et al. developed a method for detecting road from color image. Their model was performed by the aid of likelihood classification, which includes illumination variations [10]. Cheng et al. developed a technique using Hough Transform to extract roads from the high-resolution SAR image that were modeled by dark areas of parallel border. Dark areas were extracted from the image using Gaussian probability

based iterative segmentation. Then, the road was detected by Hough transformation [11]. Kong et al. generated a method called Locally Adaptive Soft-Voting (LASV). They estimated vanishing point and generated a high confidence-voting schema by Gabor Filter for detecting roads [12]. Huval et al. extracted the borderlines of the roads using Density-Based Spatial Clustering of Applications with Noise (DBSCAN). Then, they found vehicles on the road by using Convolutional Neural Networks [13]. Fritsch et al. detected road combining visual and spatial information. The visual and spatial features were employed in their study which demonstrated determining the road by means of similar road images located on spatially different places [14]. Karaduman et al. generated a method for detecting curved roads. Images were captured by the front and rear cameras for multi-view estimation. Bend direction and risk status were calculated by adding the road geometry clues [15]. Tighe et al. exploited from Super Pixel Mapping and Markov Random Field methods detecting objects in semantic and geometric classes [17]. While some of the studies that use aerial images aim object detection [25, 26, 30, 31], others detect road area [8, 11, 24, 27–29, 32–36]. Kanistras et al. conducted a survey on traffic monitoring and management with UAV. As a result of their study, they said UAVs were suitable for real-time use in traffic monitoring and were less time consuming [38]. Michailidis et al. proposed a non-linear control unit based on Circulation Control (CC) for longitudinal flight. In their study, they estimated the changes of aerodynamic coefficients, which were difficult to detect with their mathematical formulas. In the simulation table, the proposed control scheme is considered appropriate [39]. Li et al. performed this operation with genetic algorithm according to the requirements of the route planning. A simulation was realized by this study. According to the results obtained, the genetic algorithm achieved some calculations having high precision [40]. Yang et al. investigated the collision detection and resolution (CDR) of air collisions in UAVs by graph theory. They then combined the stochastic parallel gradient descent (SPGD) method and the sequential quadratic programming (SQP) algorithm to solve the problem transformed into a nonlinear optimization. They solved the problem by converting it to a two-layer optimization method [41]. Zhou et al. used Gaussian Mixture Models (GMMs). Later, the identified route was traced [42]. Lin et al. employed the histogram-based adaptive threshold method to detect the road area, and the probabilistic HT, and the clustering method were combined to segment the road [43].

Various path tracking methods have been proposed for the systems in which non-linear dynamic movements can occur. One of these methods is that of Flores et al. In this work, a method is suggested for tracking by a mini-flying vehicle. In their study, scenarios have been determined and Lyapunov based switch control method has been proposed for the follow-up of the road. The position of the vehicle with their method is stabilized [44].

In the proposed approach, KNN and HT are combined in road detection process. The results of each method are validated. Then spatial and spectral fusion are conducted, road area is classified, and then the routing mission is accomplished. Once road area is detected, the road type classification is conducted by Fuzzy approach. The proposed scheme aims to increase the correctness of route estimation.

1.5 Contribution

In this study, UAV needs a route suggestion rather solely detecting road portion pixels. For this reason, we have focused on estimating road direction. In other words, this work develops an aerial route-planning model. If we were interested in only road fields, we would just focus on HT or KNN. However, individual results of both algorithms are obtained, which refer to road segments. To find UAV

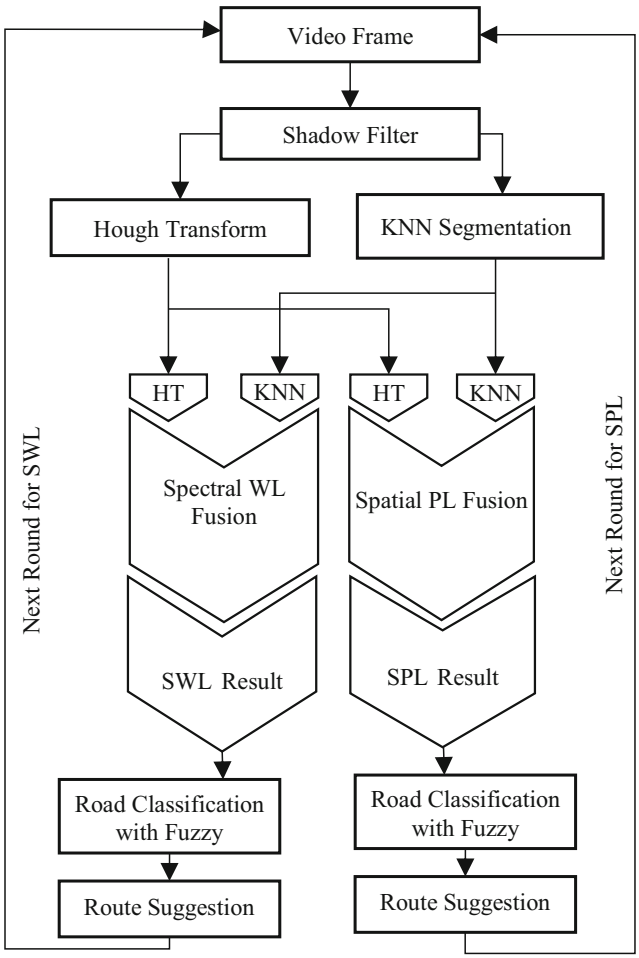

Fig. 1 The system diagram of the proposed approach

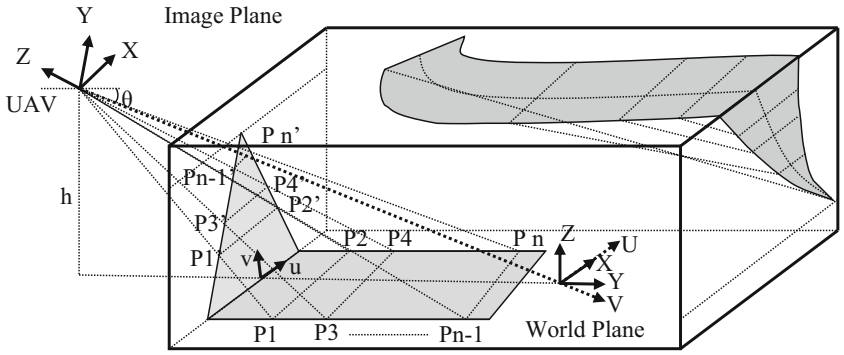

Fig. 2 Image plane and the world plane views for straight road and curved road

movement direction, results of both methods are combined by spatial and spectral fusion schemes. The intersection area is involved in the process to find direction. Before finding direction, road type is classified by Fuzzy method. Thus, we suggest a route UAV to follow. This approach reduces failure rate for getting lost as flying over curved roads. On the other hand, UAV doesn't need to recalculate return route while patrolling. This situation decreases estimation cost and provides energy saving.

1.6 Outline of the Paper

In the next Section, the proposed approach is expanded in detail. Initially, a system diagram is developed to expose the underlying theory. In the subsequent portion of this section, each step is analytically explained. In the Section 3, road detection results are given in sample frames. A reader can find error analyses and performance comparisons in the proceeded paragraphs of the section. Eventually, the final section discusses concluded results at the end of the simulation stage. Also, the future work is introduced.

2 System Theory

A system is designed for road detection and route determination, which is implemented on aerial images captured by UAV camera. The system diagram of the proposed method is given in Fig. 1. In accordance with the proposed algorithm, it is assumed that UAV is initially deployed at the start point of the subject road. Then, UAV starts capturing aerial images as soon as it comes to a specified altitude after taking perpendicularly off. These assumptions limit the underlying problem clarifying the simulation by means of anonymous experimental videos.

Therefore, aerial image frames are received as inputs. Video frames are consecutively taken with regular intervals. The frequency of this operation should be changed according to the flight speed of the UAV. For example, if the UAV flies along the road at higher speed than the specified one, capturing time period of frames should be adapted to decrease. Otherwise, it may not capture some of successive road portions, and UAV cannot correctly follow the road.

Let's imagine the opposite case in which UAV progresses in slow motion. Stand by duration after completion moment of UAV image processing should be increased, due to avoiding of duplicate processing of same frame.

To beware of experiencing such problems, image capturing frequency should be tuned according to UAV actual speed. Thus, the UAV is motivated to perform optimum number of operation providing less energy cost. The image capturing frequency is calculated by means of UAV actual speed as

$$\mathcal{T} = d / \mathcal{V}, \quad d = \Delta\xi = \mathcal{p}_e - \mathcal{p}_s \tag{1}$$

where $\mathcal{T}$ is the image capturing frequency, d is the displacement $(\Delta\xi)$ between the start location point $(\mathcal{p}_s)$ at the

(a) (b)

Fig. 3 Road image appearance for **a** the image plane; **b** the world plane

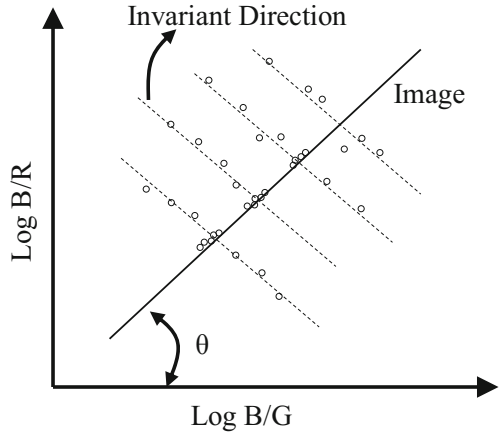

Fig. 4 Best representation of direction for minimum entropy adapted by [3]

moment of current capture and the next location point ($\mathcal{P}_e$) at the moment of subsequent image capture, and $\mathcal{V}$ is the actual speed of UAVs.

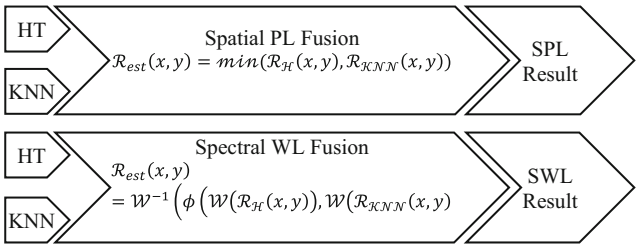

Fig. 6 Road segment detection by the proposed approach

In the world plane, the borderlines of road images are in parallel. On the other hand, perspective geometry is a bit different from the world plane view.

Here, the border lines in the road image result in two rays representing vanishing lines that intersect at the vanishing point. Therefore, the resultant perspective indicates triangle geometry for the straight roads. This situation is sketched in Fig. 2 involving the conversion between the world and the image plane. World and image plane appearance of the road is given in Fig. 3. Projective transformation for a point on

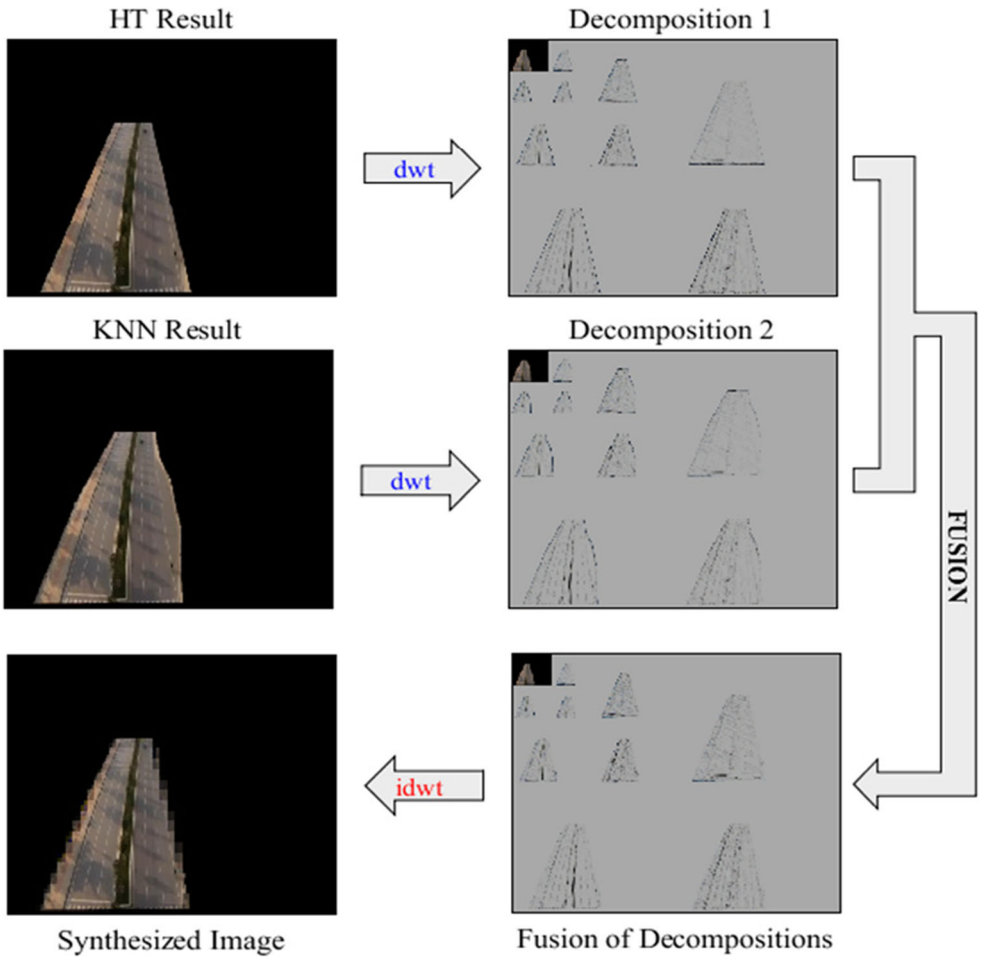

Fig. 5 Applying the Wavelet transform to the results of KNN and HT and obtaining the result of fusion

Table 1 Road type for detected area

Label	Road Type
T1	Straight
T2	Left Curved
T3	Right Curved
T4	Intersection

world plane is expressed by $\mathcal{P}' = \hbar \cdot \mathcal{P}$, where $\mathcal{P}$ refers to a point, and $\hbar$ is the homogeneous matrix [22]. This equation can be expanded by

$$\begin{pmatrix} \mathcal{P}_1' \\ \mathcal{P}_2' \\ \mathcal{P}_3' \end{pmatrix} = \begin{bmatrix} \hbar_{11} & \hbar_{12} & \hbar_{13} \\ \hbar_{21} & \hbar_{22} & \hbar_{23} \\ \hbar_{31} & \hbar_{32} & \hbar_{33} \end{bmatrix} \begin{pmatrix} \mathcal{P}_1 \\ \mathcal{P}_2 \\ \mathcal{P}_3 \end{pmatrix} \tag{2}$$

where $\hbar_{ij}$ is values of homogeneous matrix elements; the points $\mathcal{P}_1$, $\mathcal{P}_2$, and $\mathcal{P}_3$ lie on the same line in the world plane; and new points $\mathcal{P}_1'$, $\mathcal{P}_2'$, and $\mathcal{P}_3'$ lie on the same line in image plane. A point in the world plane represented by (x, y) is expressed in the image plane by (u, v). The coplanar points of world plane $\mathcal{P}_1$, $\mathcal{P}_2$, $\mathcal{P}_3$, and $\mathcal{P}_4$ are shown in image plane by $\mathcal{P}_1'$, $\mathcal{P}_2'$, $\mathcal{P}_3'$, and $\mathcal{P}_4'$ as shown in Fig. 2. In the world plane, the road border lines are parallel, which are the line segments $\overline{\ell_{\alpha_1}}, \overline{\ell_{\beta_1}}$ bounded by two distinct end points $\mathcal{P}_1, \mathcal{P}_3$ and $\mathcal{P}_2, \mathcal{P}_4$. In the image plane, however, road borders are not parallel which are the line segments $\overline{\ell_{\alpha_1}}, \overline{\ell_{\beta_1}}$ bounded by two distinct end points $\mathcal{P}_1', \mathcal{P}_3'$ and $\mathcal{P}_2', \mathcal{P}_4'$ due to its perspective view geometry.

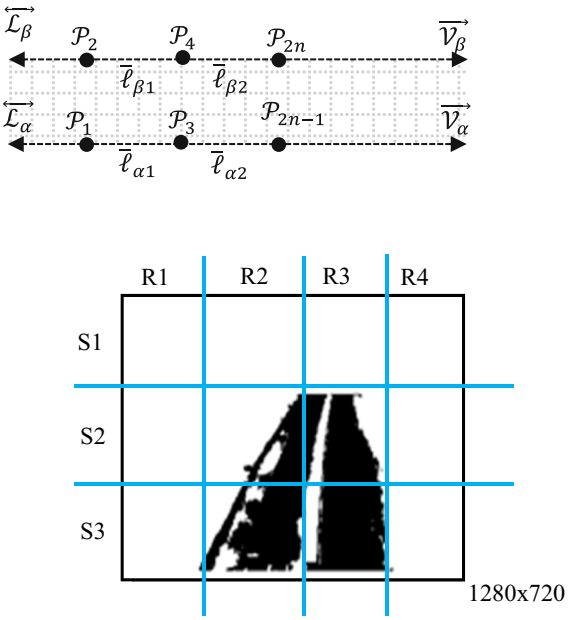

Fig. 7 Segmented detected road area

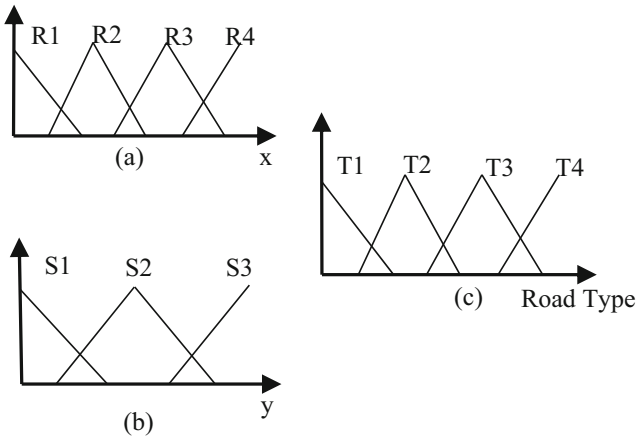

Fig. 8 **a** and **b** are membership functions for input variables, **c** is output of the Fuzzy Classifier

Provided that $\overleftrightarrow{\mathcal{L}_\alpha} \parallel \overleftrightarrow{\mathcal{L}_\beta}$

$$\overline{\ell_{\alpha_n}} = \left\{ [\mathcal{P}_a, \mathcal{P}_b] \mid a, b \in \{1, 3, .., 2n-1\}, n \in \mathbb{Z} \right\}$$
$$\overline{\ell_{\beta_n}} = \{ [\mathcal{P}_c, \mathcal{P}_d] \mid c, d \in \{2, 4, .., 2n\}, n \in \mathbb{Z} \}$$

where $[\mathcal{P}_a, \mathcal{P}_b]$ refers to the line segment represented by $\overline{\ell}_{\alpha_n}$; $\overleftrightarrow{\mathcal{L}_\alpha}$, $\overleftrightarrow{\mathcal{L}_\beta}$ denote to the border lines, and $\overrightarrow{\mathcal{V}_\beta}$, $\overrightarrow{\mathcal{V}_\alpha}$ are the road border vectors.

To estimate UAV route after detecting the road, aerial images portions are employed. Before Hough Transformation based road detection, initially, color conversion is applied to the image, since the UAV in-motion through the air may suffer from distorted images. Gaussian filter is used to eliminate distortion and noise. The next step is to apply edge detection process addressed by well-known Sobel method. Road image segmentation is achieved by means of detected edges. Both borders of the road are detected by HT which was originally developed to find straight and circle like lines in an image. Therefore, the first input to the fusion stage is obtained. When the HT method cannot detect the road area in the curved roads, the road to the KNN method is regarded as the result. KNN based road detection in the image may accommodate shadows, due to the illumination effect over possible man-made or natural objects surrounding subject road. Different color tones on the road image may refer to possible shadows that may cause failure

Table 2 Rule table for Fuzzy Classifier

y	R1	R2	R3	R4
S1	0	0	0	0
S2	T2	T1	T1	T3
S3	T4	T1	T1	T4

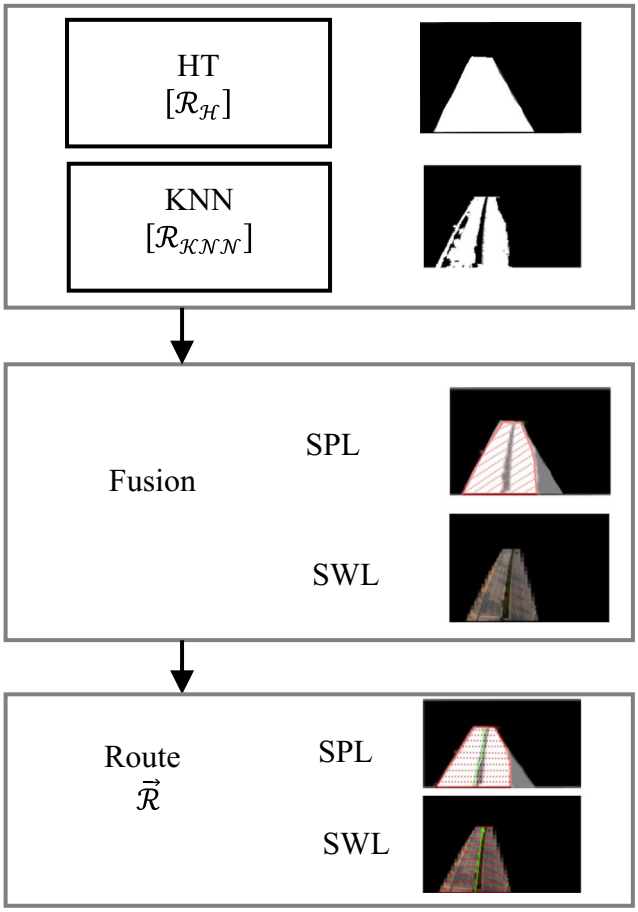

Fig. 9 Route estimation followed by road detection

while conducting image segmentation. Therefore, the elimination of shadows from RGB image is required. To suppress shadows, minimum entropy method is applied to the subject road image [3]. First step is to calculate the geometric average of RGB color channels, which can be written as $\mathcal{G} = \sqrt[3]{\mathcal{P}_{\mathcal{R}} \cdot \mathcal{P}_{\mathcal{G}} \cdot \mathcal{P}_{\mathcal{B}}}$ where $\mathcal{G}$ denotes to geometric average, and $\mathcal{P}_{\mathcal{R}}$, $\mathcal{P}_{\mathcal{G}}$, $\mathcal{P}_{\mathcal{B}}$ refer to color values for each pixel of the subject image. This situation can be expressed by

$$c_k = \begin{cases} 1 & \mathcal{P}_{\mathcal{R}} \cdot \mathcal{P}_{\mathcal{G}} \cdot \mathcal{P}_{\mathcal{B}} = 0 \\ \mathcal{M}/\mathcal{G} & \mathcal{P}_{\mathcal{R}} \cdot \mathcal{P}_{\mathcal{G}} \cdot \mathcal{P}_{\mathcal{B}} > 0 \end{cases} \Bigg| \begin{array}{c} 0 < \mathcal{R}, \mathcal{G}, \mathcal{B} < 256 \\ \mathcal{M} \in \{\mathcal{R}, \mathcal{G}, \mathcal{B}\} \; k \in \{1, 2, 3\} \end{array} \tag{3}$$

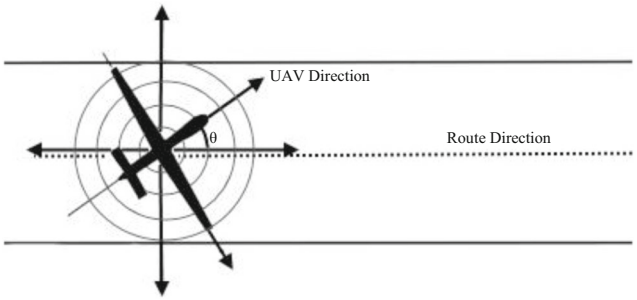

Fig. 11 Sketching UAV routing

where $\mathcal{M}$ is the color values, taking $\mathcal{R}, \mathcal{G}, \mathcal{B}$, for subject pixel, $\mathcal{G}$ is geometric average of subject pixel, and c is the resultant value. c value is calculated for each color channel (c_1, c_2, c_3 for $\mathcal{R}, \mathcal{G}, \mathcal{B}$, respectively). Thus, $\mathcal{N}_{11}$, $\mathcal{N}_{21}$ values are obtained by $\mathcal{N} = U \log(c_k)$ where U indicates a matrix of 2x3, and $\mathcal{N}$ denotes to a matrix of 2×1 [3].

Figure 4 illustrates the invariant direction for the image. The final step of the shadow detection stage is to find correct projection angle substituted in

$$I = \mathcal{N}_{11} \cos\theta + \mathcal{N}_{21} \sin\theta \tag{4}$$

where I refers to gray image without shadow. The following stage is the entropy calculation which is $H = -\sum_i p_i(I) \log(p_i(I))$. The result can be assessed by

$$I = \{\theta |\; argmin(H), 0 \leq \theta \leq 180 \tag{5}$$

Equation 5 aids to find θ angle involving in the minimum entropy calculation. Consequently, possible shadows are all removed from the subject image [3]. After many trials are experimented, most proper threshold rate is determined to convert the image into black and white. Image segmentation is accomplished by KNN. The training set is arranged. Then, the similarity rate between the pixels to be classified and the pixels in training set is calculated. And then, the average value of the nearest ones to the pixels to be classified is calculated. The raw pixels are assigned to the specified classes considering threshold values. Here, class features play important role in the performance of the present process, which are the number of nearest neighbors, threshold value, and similarity measure. The Euclidean

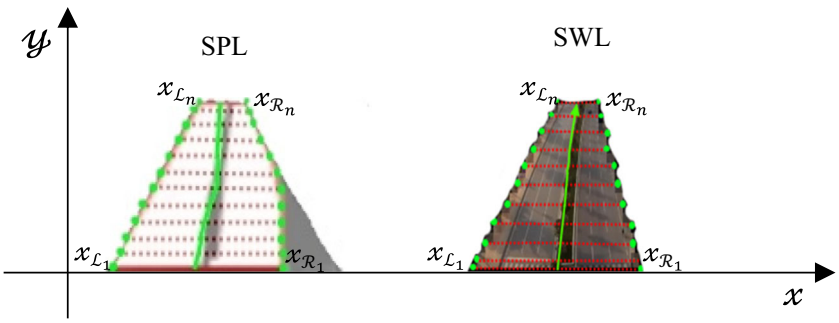

Fig. 10 Sketching raster processing for determination of the end points on the road borders as estimating route

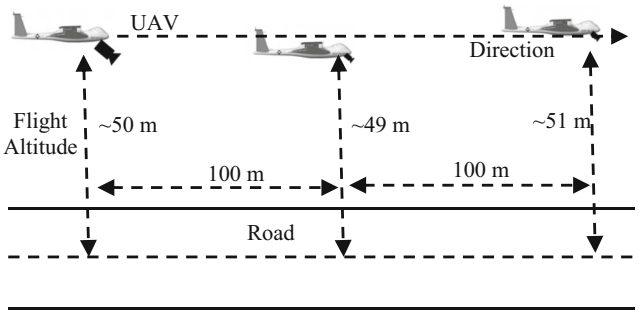

Fig. 12 Representation of UAV height and direction

distance between specified points is obtained by

$$d = \sqrt{(p_x - q_x)^2 + (p_y - q_y)^2} \tag{6}$$

where d is the calculated distance, p and q are subject pixels in the image (Fig. 5).

Conventionally, the aim of image fusion is to get a useful result in a unique image combining multi-sensory images. Image fusion can be classified in three folds: object level, feature level, and pixel level (PL). Pixel level image fusion is employed by the present study because of its simplicity. Pixel level fusion increases the useful information content of an image [23]. Pixel level methods may include arithmetic, color, and multi resolution signal fusion. Simple mathematical processes using pixel values are applied for arithmetic methods getting involved in calculations of average, minimum, maximum values, and etc. In the color fusion methods, specified conversions using color channels are conducted. Well-known Intensity Hue Saturation (IHS) method is aimed to get spatial features of RGB images.

In the Signal level multi resolution methods, subject image is decomposed to sub-bands, and running the fusion loop. Further, Wavelet scheme is a good example for the present problem. Here, the image is decomposed to sub images having different resolutions. Wavelet based fusion selects salient features of input images, and then combines them to increase the useful information content of the subject image. While selecting salient features, both spatial and spectral components of subject image have to be maintained.

In this study, two processed images via KNN and HT are found. Then, intersection area indicating road segment is extracted by the PL fusion method as shown in Fig. 6.

The route type must be specified before the route is determined. Road types are given in Table 1. The type of road is determined by using Fuzzy Classifier. Certainly, calculations are made by means of membership functions and rules. Hence, the route is determined, which is the direction of UAV to continue. The type of route of the UAV is taken into consideration. Figure 7 shows the image sections for the Fuzzy Classifier. The horizontal divisions are denoted by S, and the vertical divisions by R. Figure 8 shows membership functions and output values for Fuzzy Classifier. Input values for Fuzzy Classifier are shown in (a) and (b), and output value is shown in (c) of Fig. 8.

The rule table for the Fuzzy Classifier is shown in Table 2.

Spatial and spectral fusion stages are shown in Fig. 9. The result obtained by the Fusion is correlated to suggested route which can be calculated as

$$\vec{\mathcal{R}}(x) = \frac{x_{\mathcal{L}} + x_{\mathcal{R}}}{2} \tag{7}$$

$$x_{\mathcal{L}} = \forall y, \min(x), \mathcal{P}(x, y) = 1 \mid \forall \mathcal{P} \in \mathcal{R}$$
$$x_{\mathcal{R}} = \forall y, \max(x), \mathcal{P}(x, y) = 1 \mid \forall \mathcal{P} \in \mathcal{R}$$

where x refers to horizontal location of binary image, y denotes to vertical location of binary image, and $\mathcal{L}, \mathcal{R}$ indicate left and right side of the road, respectively.

Estimated route is sketched in Fig. 10. Each horizontal line represents the raster lines of the resultant image. Minimum and maximum points on same raster line are replaced in Eq. 7. Calculated result finds the location of the pixel towards where UAV should move. Hence, all the route pixels are estimated line by line.

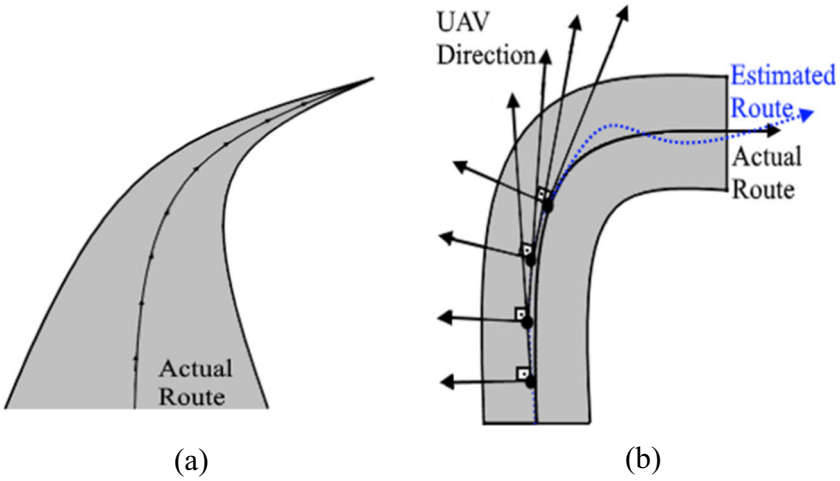

Fig. 13 **a** Route appearance on perspective image; **b** Correcting UAV directions for curved road on world plane

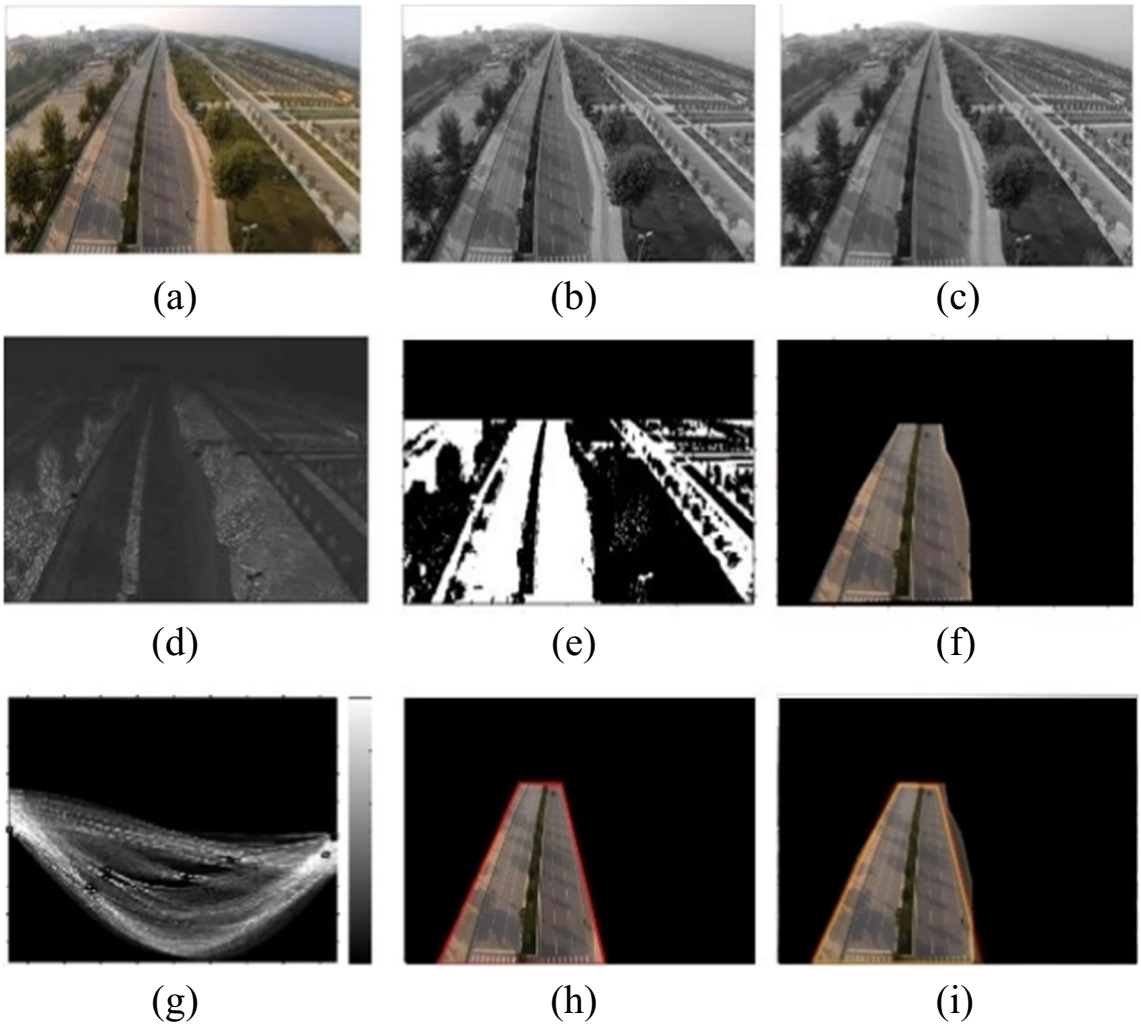

Fig. 14 **a** Subject road image; **b** Gray level image; **c** The image with filter; **d** The image without shadow; **e** Thresholded image; **f** KNN result; **g** HT edge map plot; **h** HT result; **i** PL fusion result

Current UAV direction and the suggested route direction are simulated in Fig. 11. Current direction of UAV should overlap with the estimated route. In this manner, UAV can follow the suggested route.

The UAV in the experiment flies at nearly a fixed altitude of 50 m, which is illustrated in Fig. 12. Hence, the frames were used as uncalibrated images due to the fixed flight position of UAV.

Fig. 15 Some of the sample road detections

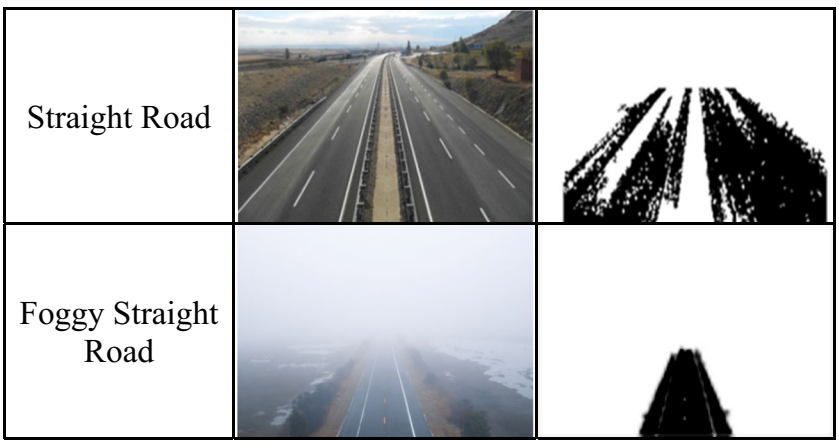

Table 3 Success rates for the methods

	SPL	SWL	KNN	HT
Success Rate (%)	99.00	99.00	96.00	92.0
Total Images (Item)	100	100	100	100

The UAV sometimes flies at a deviated up/down altitude level of a few meters that is negligible for the proposed approach as tracking the road using uncalibrated camera. As the UAV progresses along the route it can update its existing route giving new angles just after every displacement points as sketched in Fig. 13.

$$Loop = \begin{cases} m_{UAV} = m_{UAV}, m_{UAV} - m_R = 0 \\ m_{UAV} = m_{UAV} + 1, m_{UAV} - m_R < 0 \\ m_{UAV} = m_{UAV} - 1, m_{UAV} - m_R > 0 \end{cases} \quad (8)$$

The resultant road segment is provided in Fig. 14-i. Finally, the suggested route UAV to follow is estimated. Image capturing frequency is determined according to UAV speed and calculation time. In this manner UAV keeps moving over the road running the same loop.

UAV have to wait for a minimum delay time which is the sum of capturing time and estimation time as

$$t_d = t_c + t_p \quad (9)$$

where t_d refers delay time, t_c represents capture time, and t_p denotes to estimation time.

2.1 Error Analysis

Root Mean Square (RMS) error rates for the performance results are evaluated by $\mathcal{E}_{rms} = \sqrt{(1/n)} \cdot \sum_{i=1}^{n} \mathcal{X}_i^2$ where n refers to total number of images, $X$is error for per detection, and $\mathcal{E}_{rms}$ represents total error rate. Moreover, receiving operating characteristic (ROC) is benefited to get the performance for 100 images.

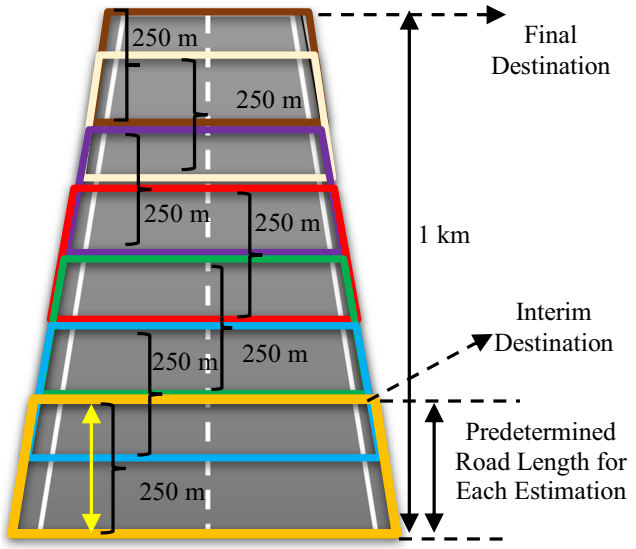

Fig. 16 Simulation of road area detection for 1 km straight road

Table 4 Estimation time for the proposed method, and distance taken for UAV flight

Estimation time (sec.)	Progressed road length during estimation time (meter)	UAV speed (km/h)	Predetermined road length for each estimation (meter)
1.20	16.67	50	250
1.05	14.58	50	250
0.75	10.42	50	250
0.21	2.92	50	250

3 Simulation Results

In the simulations, 100 different anonymous aerial road images and an anonymous UAV video stream of 1 km road are experimented. Two different methods are proposed in the road detection stage of our algorithm, which are KNN and HT.

Road segments are detected by using the algorithm as shown in Fig. 15. The black region refers to the road segment detected by the proposed method, thereafter determining the type of road by Fuzzy Classifier The route is calculated after the road area is detected. This calculation is performed by Eq. 7. The picture on the bottom side of Fig. 15 is a sample one for foggy straight road. Here, the visibility distance is getting shorter as seen more clearly in the segmented image. In fact, we do not deserve drone to fly under heavy weather conditions.

The road images obtained by the results of both methods are simply intersected to increase suggested route accuracy rate. If the intersected area is under 65%, the same loop runs once more until the resulted area becomes over the specified rate that is experimentally obtained. Success rate is obtained by percentage of correctly detected road images out of 100

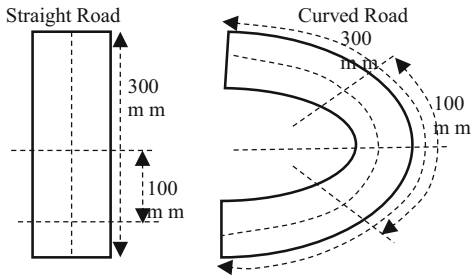

Fig. 17 Simulation of straight and curved road area

subject images. The intersection result of both algorithms is 99.00% which outperforms the results of KNN and HT, given in Table 3.

Determination of the road area for 1 km road is shown in Fig. 16. Each detection is made for a 250-meter road. The UAV calculates the distance to travel again after traveling 100 m over the road. New road area is detected, and route is determined again. Hence, simulated UAV can continue to follow the route. Delay time is calculated by Eq. 1.

Table 4 shows the estimation time for the proposed approach. Repetition frequency of each estimation is 10 per 1 km. In other word, same estimation process is renewed for each interval corresponding to 100m. In the straight roads, this interval could be given greater than 233m, which is calculated as 250-16.67≈233m.

However, UAV view distance is getting less for curved roads, as seen in Fig. 17. Aforementioned interval may decrease according to sharpness of that bend. If we assume

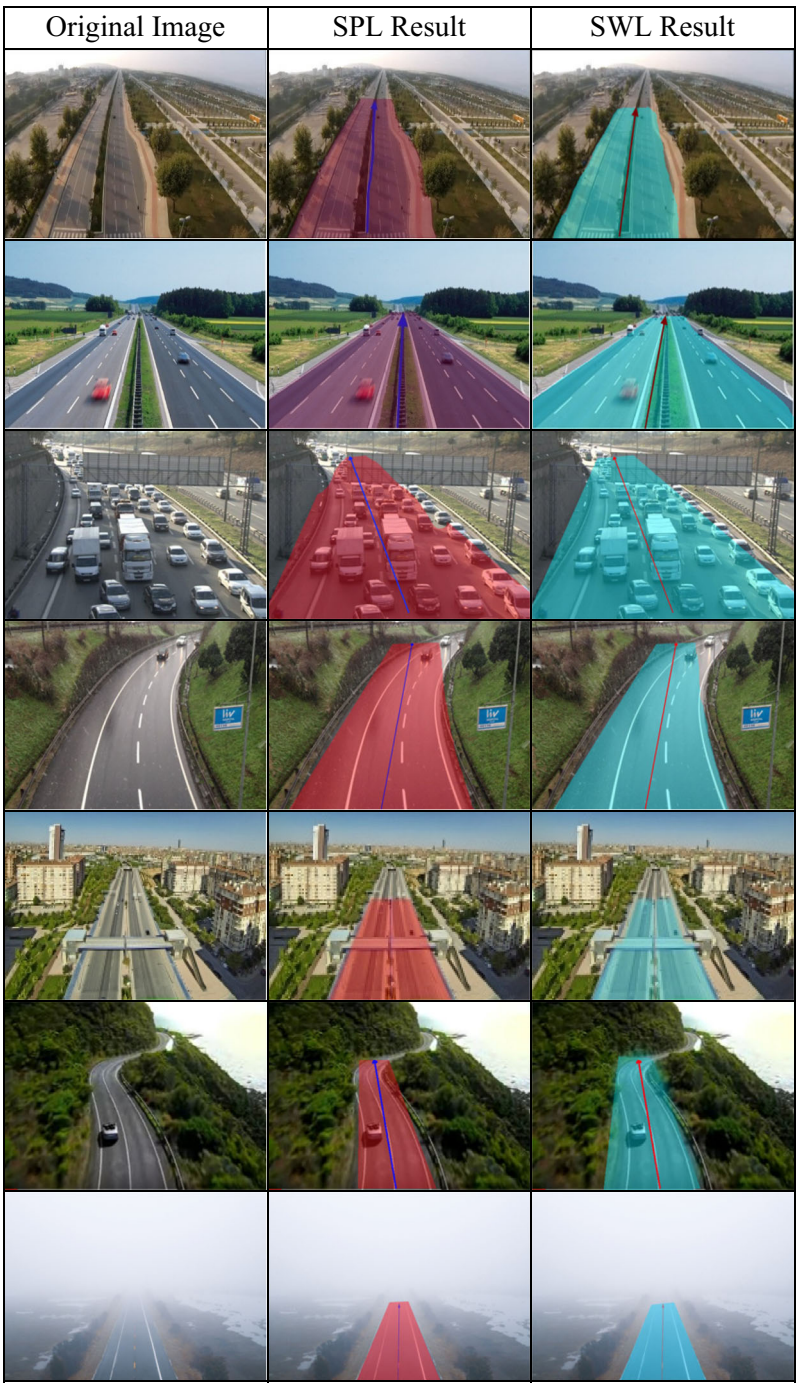

Fig. 18 Some of the sample road detection and route estimation results

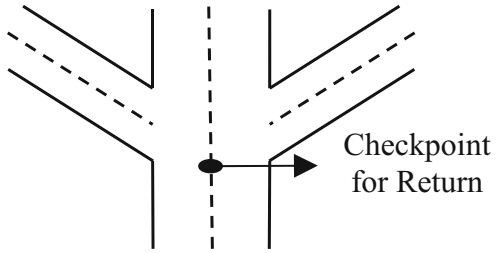

Fig. 19 Determination of direction and checkpoint in complex roads

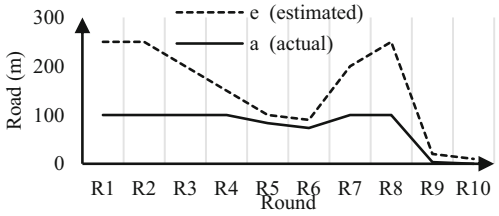

Fig. 21 Estimated versus actual road distances for next round image detection

that UAV comes over a sharp bend calculation interval should be much reduced than that of straight road (Fig. 18).

In order to cover all types of road shapes the calculation interval is intuitively taken as 100m [37].

$$a = \begin{cases} 100 & e > 100 \\ e - 16.67 & 16.67 < e < 100 \\ 0 & e < 16.67 \end{cases} \tag{10}$$

where a denotes actual distance taken from present estimation point to the next one; and e represents estimated distance from existing point to interim destination point.

In the proposed simulation study, it is assumed that the UAV follows a straight or curved road portion with light or heavy traffic as shown in Fig. 18. This solution does not cover every kind of roads. Because our scenario refers to patrolling over assigned noncomplex roads. For that reason, the situations seen in Fig. 20 is not in the scope of this work. As an example, in the case of intersections, the route to follow should be decided. To exemplify aforementioned situations, a sample complex road scenario is sketched in Fig. 19. A checkpoint location is assigned for this case. UAV may decide its direction once it reaches the checkpoint. Some examples of complex roads and the results are provided in Fig. 20.

Equation 10 defines specifying interim destination points to capture frames along the final destination point. Figure 21 indicates estimated distances versus actual road distances for each interim destination points. Once UAV reaches to interim destination point, next one is recalculated.

This task is progressively repeated by the final destination point. Therefore, especially for curved road, this approach minimizes potential risk UAV to deviate from the specified road. One of the performance criteria is the pixelized road detection rate which is calculated by

$$\psi_d = \frac{1}{n} \cdot \sum_{i=1}^{n} d_i \tag{11}$$

where ψ_d is average number of road pixel, n is total images and, d is rate of detected road pixels for road image. Another one is the error rate for detected pixels which can be given as

$$\psi_e = \frac{1}{n} \cdot \sum_{i=1}^{n} e_i \tag{12}$$

where ψ_e is average error rate, n is total number of images, and e is the error rate for detected road pixels.

Different performance plots are given in Fig. 22. The resultant KNN and HT detection rate for road area pixels are respectively 98.10%, 97.04%, and fused detection result

Fig. 20 Complex road samples with checkpoints

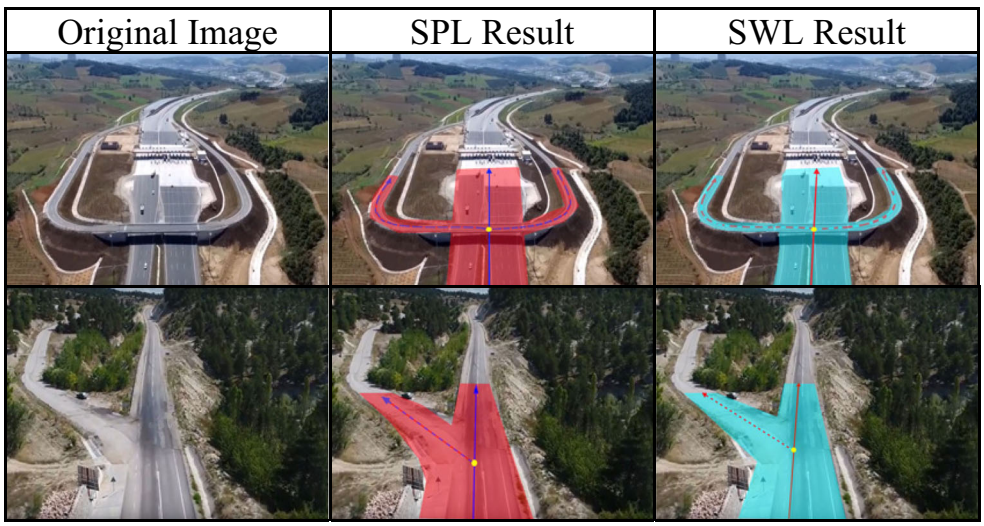

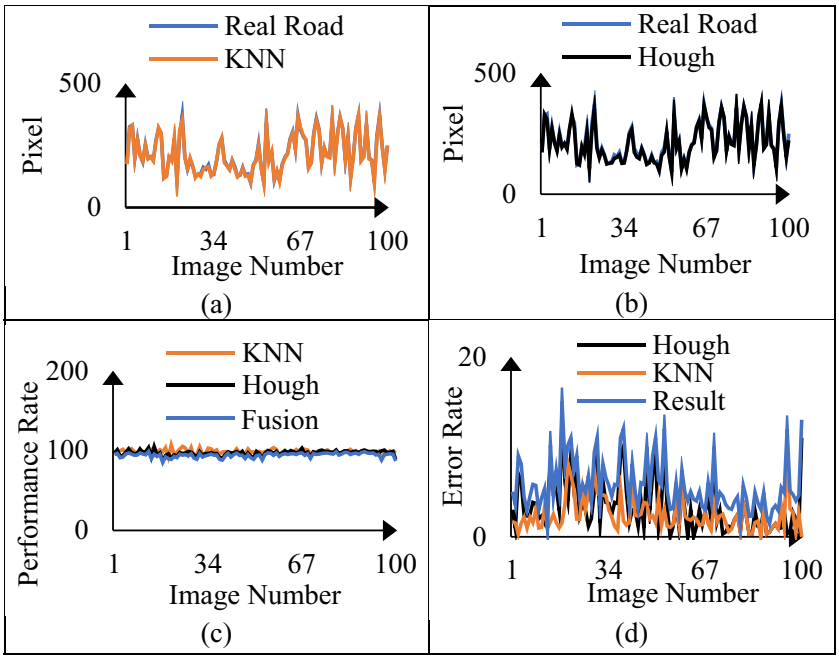

Fig. 22 **a** Detected pixels by KNN; **b** Detected pixels by HT; **c** Performance rate; **d** Error rate

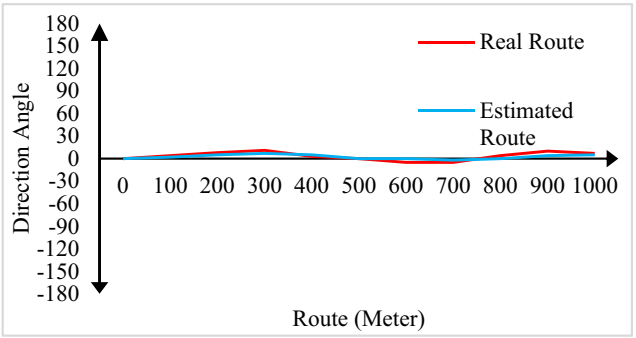

Fig. 23 Deflection angles between current UAV route and estimated one for the simulated 1 km-road

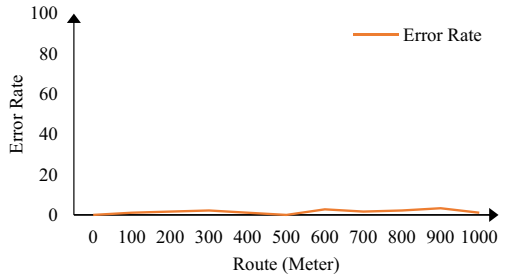

Fig. 24 Deflection angles error between current UAV route and suggested one for the simulated 1 km-road

rate becomes 95.40%. These estimated rates represent proportional rates of road portion pixels in question.

Here, proportion of detected road pixel rate decreases while probability rate for accurate detection of road increases, since the result obtained by the proposed fusion method represents intersected pixels. Therefore, the probability rate for road detection is 96% for KNN, 92% for HT, and it becomes 99% for the proposed approach.

Figure 23 gives the actual direction and the direction angle values for the calculated route. The starting direction was accepted as zero, and accordingly the angle was calculated for the new direction at the end of every 100 m.

Figure 24 gives the error rate between the actual route and the calculated route.

In other words, average error rate for KNN, HT and FR comes out respectively 1.90%, 2.96%, and 4.60%. 1 km road process error result for deflection angles between current UAV route and suggested one is plotted in Fig. 23.

Table 5 Estimation time for the different sizes of images

No	Image Size (pixel)	Spatial Est. Time (sec.)	Image Size (pixel)	Spectral Est. Time (sec.)
1	1280 × 720	1.20	720 × 720	1.80
2	800 × 600	1.05	600 × 600	1.44
3	640 × 480	0.75	480 × 480	1.10
4	320 × 200	0.21	200 × 200	0.41

Table 6 Performance comparisons

Studies	Method	Database	Performance (%)
Alvarez and Lopez [10]	Likelihood Based Classi?er and Illuminant-Invariant	Cvc-cer-01	90.00
Brostow et al. [18]	Semantic Segmentation	Their own data	89.50
Ladicky et al. [19]	Conditional Random Field	CamVid	93.90
Zhang et al. [20]	Depth Maps	CamVid	98.50
Sturgess et al. [21]	Conditional Random Field	CamVid	95.30
Lin and Saripalli [8]	Histogram-Based Adaptive Threshold	Their own data	99.88
Tighe and Lazebnik [17]	Nearest-Neighbor Superpixels, MRF	SIFT Flow	96.20
Gould et al. [16]	Unified Energy Function	Geometric Context	86.90
Sommer et al. [25]	Object Proposals Methods	DLR 3K Munich	95.00
Geiger et al. [36]	Slam	KITTI	97.80
Zhou et al. [42]	Graph Cut Based Methods	Their own data	99.45
Lin and Saripalli [43]	Histogram, HT, Naive–Bayes Classifier	Their own data	96.00
Proposed Approach	KNN-HT	Anonymous images and video stream	99.00

Table 5 comprises some of the results for the different sizes of images.

The existing trials are experimented for the 1 km road and its success rate reaches up to 99%. Performance rate of similar studies for different road database are provided in Table 6.

4 Discussions and Conclusions

Some assumptions have been taken by the proposed approach. The UAV is considered to be moving at a fixed altitude and the speed is 50 km/h. It is assumed that the start and end points of the UAV are known. This work was achieved by an anonymous streaming video captured from UAV for simulation purposes.

Fig. 25 Experimental UAVs to produce our own aerial images and video data

In this study, we have aimed to determine UAV route in an effective way. The results of two detection algorithms have been fused to suggest a direction for UAV. In fact, this is a 2 dimensional route-planning scheme. According to the performance rates, spatial and spectral fusion give equivalent results except higher process time of PL fusion. The present paper is supported by the other research studies in comparison concern. As a future work, we will assign our own UAV aerial video stream. For that reason, we have already arranged a laboratory as shown in Fig. 25. Using our own UAV aerial image and video database, we are planning to detect aerial obstacles. To bring a UAV maneuver capability in Z-axis, perpendicular coordinate is supported by depth map. In this way, three dimensional path planning will be conducted. As a final word, it is not difficult to foresee, human being will thoroughly cope with numerous autonomous flying problems over next decades.

References

1. Federal Aviation Administration (FAA), http://www.faa.gov (2017)
2. Ehang, Homepage: http://www.ehang.com/ehang184 (2017)
3. Finlayson, G.D., Drew, M.S., Lu, C.: Intrinsic images by entropy minimization. In: Computer Vision-ECCV 2004, pp. 582-595. Springer, Berlin (2004)

4. He, Y., Wang, H., Zhang, B.: Color based road detection in urban traffic scenes. Intell Trans Syst IEEE **1**, 730- 735 (2003)
5. Wang, Y., Teoh, E., Shen, D.: Lane detection and tracking using b-snake. Image Vis Comput **22**(4), 269–280 (2004)
6. Broggi, A.: Robust real-time lane and road detection in critical shadow conditions. In: Proceedings IEEE International Symposium on Computer Vision, pp. 353–358 (1995)
7. Kong, H., Audibert, J.Y., Ponce, J.: Vanishing point detection for road detection. In: Proceedings IEEE Conference Computer Vision Pattern Recognition, pp. 96–103 (2009)
8. Lin, Y., Saripalli, S.: Road detection from aerial imagery. In: 2012 IEEE International Conference on Robotics and Automation (ICRA), pp. 3588–3593 (2012)
9. Fernandez, C., Izquierdo, R., Fernandez Llorca, D., Sotelo, M.A.: A comparative analysis of decision trees based classifiers for road detection in urban environments. In: 2015 IEEE 18th International Conference on Intelligent Transportation Systems (ITSC), pp. 719–724 (2015)
10. Alvarez, J.M., Lopez, A.M.: Road detection based on illuminant invariance, vol. 12 (2011)
11. Cheng-Li, J., Ke-Feng, J., Yong-Mei, J., Gang-Yao, K.: Road Extraction from High-Resolution SAR Imagery Using Hough Transform. In: IEEE International Geoscience and Remote Sensing Symposium, IGARSS'05. vol. 1, pp. 4-pp, IEEE (2005)
12. Kong, H., Audibert, J.Y., Ponce, J.: General road detection from a single image. IEEE Trans. Image Process. **19**(8), 2211–2220 (2010)
13. Huval, B., Wang, T., Tandon, S., Kiske, J., Song, W., Pazhayampallil, J., Andriluka, M., Rajpurkar, P., Migimatsu, T., Yue, R.C., Mujica, F., Coates, A., Ng, A.Y.: An empirical evaluation of deep learning on highway driving, arXiv:1504.01716 (2015)
14. Fritsch, J., Kuhnl, T., Kummert, F.: Monocular road terrain detection by combining visual and spatial information. IEEE Trans. Intell. Transp. Syst. **15**(4), 1586–1596 (2014)
15. Karaduman, O., Eren, H., Kurum, H., Celenk, M.: Road-Geometry-Based Risk estimation model for horizontal curves. IEEE Trans. Intell. Transp. Syst. **99**, 1–11 (2016)
16. Gould, S., Fulton, S.R., Koller, D.: Decomposing a Scene into Geometric and Semantically Consistent Regions. In: IEEE 12th International Conference on Computer Vision, IEEE, pp. 1–8 (2009)
17. Tighe, J., Lazebnik, S.: Superparsing: scalable nonparametric image parsing with super pixels. In: Computer Vision–ECCV, pp. 352–365. Springer, Berlin (2010)
18. Brostow, G.J., Shotton, J., Fauqueur, J., Cipolla, R.: Segmentation and recognition using structure from motion point clouds. In: Proceedings European Conference Computer Vision, pp. 1–15 (2008)
19. Ladicky, L., Sturgess, P., Alahari, K., Russell, C., Torr, P.H.S.: What, Where and How Many? Combining Object Detectors and CRFs. In: Proceedings European Conference Computer Vision, pp. 424–437 (2010)
20. Zhang, C., Wang, L., Yang, R.: Semantic Segmentation of Urban Scenes using Dense Depth Maps. In: Proceedings European Conference Computer Vision, pp. 708–721 (2010)
21. Sturgess, P., Alahari, K., Ladicky, L., Torr, P.H.S.: Combining appearance and structure from motion features for road scene understanding. In: British Machine Vision Conference, pp. 1–11 (2009)
22. Hartley, R., Zisserman, A.: Multiple view geometry in computer vision. Cambridge University Press, Cambridge (2003)
23. Li, H., Manjunath, B.S., Mitra, S.K.: Multisensor Image Fusion using the Wavelet Transform. Graphical Models Image Process. **57**(3), 235–245 (1995)
24. Zhou, H., Kong, H., Wei, L., Creighton, D., Nahavandi, S.: On detecting road regions in a single UAV image. IEEE Trans. Intell. Transp. Syst. **18**(7), 1713–1722 (2017)
25. Sommer, L.W., Schuchert, T., Beyerer, J.: A comprehensive study on object proposals methods for vehicle detection in aerial images. In: 9th IAPR Workshop on Pattern Recogniton in Remote Sensing (PRRS), pp. 1–6 (2016)
26. Xu, Y., Yu, G., Wu, X., Wang, Y., Ma, Y.: An enhanced Viola-Jones vehicle detection method from unmanned aerial vehicles imagery. IEEE Trans. Intell. Transp. Syst. **7**, 1845–1856 (2017)
27. Elliethy, A., Sharma, G.: Automatic registration of wide area motion imagery to vector road maps by exploiting vehicle detections. IEEE Trans. Image Process. **25**(11), 5304–5315 (2016)
28. Trinder, J.C., Wang, Y.: Automatic road extraction from aerial images. Digi. Signal Process. **8**(4), 215–224 (1998)
29. Barkley, B.E., Paley, D.A.: Cooperative bayesian target detection on a real road network using aerial vehicles. In: International Conference on Unmanned Aircraft Systems (ICUAS), pp. 53–61 (2016)
30. Liu, K., Mattyus, G.: Fast multiclass vehicle detection on aerial images. IEEE Geosci. Remote Sens. Lett. **12**(9), 1938–1942 (2015)
31. Qu, Y., Jiang, L., Guo, X.: Moving vehicle detection with convolutional networks in UAV videos. In: 2nd International Conference on Control, Automation and Robotics (ICCAR), pp. 225–229 (2016)
32. Zhou, H., Kong, H., Wei, L., Creighton, D., Nahavandi, S.: On Detecting road regions in a single UAV image. IEEE transactions on intelligent transportation systems (2016)
33. Peng, X.Z., Lin, H.Y., Dai, J.M.: Path planning and obstacle avoidance for vision guided quadrotor UAV navigation. In: 12th IEEE International Conference on Control and Automation (ICCA), pp. 984–989 (2016)
34. Karila, K., Matikainen, L., Puttonen, E., Hyyppä, J.: Feasibility of multispectral airborne laser scanning data for road mapping. IEEE Geosci. Remote Sens. Lett. **14**(3), 294–298 (2017)
35. Rasmussen, S., Kalyanam, K., Kingston, D.: Field experiment of a fully autonomous multiple UAV/UGS intruder detection and monitoring system. In: International Conference on Unmanned Aircraft Systems (ICUAS), pp. 1293–1302 (2016)
36. Geiger, A., Lenz, P., Urtasun, R.: Are We Ready for Autonomous Driving? The KITTI Vision Benchmark Suite. In: IEEE Conference on Computer Vision and Pattern Recognition (CVPR) (2012)
37. Staplin, L., Gish, K.W., Decina, L.E., Lococo, K.H., Harkey, D.L., Tarawneh, M.S., Garvey, P.: Synthesis of Human Factors Research On Older Drivers And Highway Safety, Human Factors And Highway Safety Research Synthesis, V(II) (1997)
38. Kanistras, K., Martins, G., Rutherford, M.J., Valavanis, K.P.: Survey of Unmanned Aerial Vehicles (UAVs) for Traffic Monitoring. In: Handbook of Unmanned Aerial Vehicles, pp. 2643–2666. Springer, Netherlands (2015)
39. Michailidis, M.G., Kanistras, K., Agha, M., Rutherford, M.J., Valavanis, K.P.: Robust nonlinear control of the longitudinal flight dynamics of a circulation control fixed wing UAV. In: 56th IEEE Conference on Decision and Control, pp. 3920–3927 (2017)
40. Li, L., Zhang, Y.: Route planning based on genetic algorithm. J. Math. Res. **10**(2), 122–128 (2018)
41. Yang, J., Yin, D., Shen, L., Cheng, Q., Xie, X.: Cooperative deconflicting heading maneuvers applied to unmanned aerial vehicles in Non-Segregated airspace. J. Intell. Robot. Syst. **92**(1), 187–201 (2018)
42. Zhou, H., Kong, H., Wei, L., Creighton, D., Nahavandi, S.: Efficient road detection and tracking for unmanned aerial vehicle. IEEE Trans. Intell. Transp. Syst. **16**(1), 297–309 (2015)

43. Lin, Y., Saripalli, S.: Road detection and tracking from aerial desert imagery. J. Intell. Robot. Syst. **65**(1-4), 345–359 (2012)
44. Flores, G.F., Lozano Leal, R., Sanahuja, G.: Lyapunov-Based Switching Control for a Road Estimation and Tracking Applied on a Convertible MAV. In: Proceedings AIAA Guidance, Navigation, and Control (GNC) Conference, pp. 1–13 (2013)
45. http://www.bloomberg.com/news/articles/2015-04-25/amazon-seeks-chance-to-show-u-s-drones-can-safely-deliver-cargo, 2015

Mücahit Karaduman received the B.S., degree in computer engineering from Fırat University, Elazig, Turkey in 2006, and the M.S. degree, computer engineering from Fırat University, Elazig, Turkey in 2016, and second M.S. degree from Ecoinformatics Program in the same institution in 2018. He has still been pursuing Ph.D. degree from Computer Engineering, at Inonu University, Malatya, Turkey. Since 2013, he has been working as lecturer at the Computer Science Department of Inonu University, Malatya, Turkey. He has provided contributions to many international conferences as author and presenter. He is interested in Intelligent Transportation, air traffic, and video processing.

Ahmet Çınar received the B.S., M.S., and Ph.D. degrees in electrical and electronics eng. from the Fırat University, Elazığ, Turkey in 1993, 1996, and 2003, respectively. He was the head of Informatics Department between 2007 and 2008. Since 1995, he has been working as lecturer and assistant professor at the Computer Engineering Department of Firat University, Elazığ, Turkey. He has provided contributions to many journals and international conferences as author and presenter. He is interested in mesh generation, virtual and augmented reality, image processing, human computer interaction, animation, heuristic methods, physically-based simulation, physics and game engines, GPU-based processing and programming, and computer vision.

Haluk Eren received the B.S., M.S., and Ph.D. degrees in electrical and electronics eng. from the Fırat University, Elazığ, Turkey in 1989, 2002, and 2011, respectively. He had a scholarship from World Bank, and went to MANCAD, Manchester, U.K. for industrial education project in 1993, 1994. Then, he was appointed as a lecturer in F.U., Dept. of Computer Science. In 2008, he went to Ohio University, Athens, OH with Ph.D. scholarship in dept. of EECS. In 2009, he was the post Ph.D. Researcher in OSU Photogrammetric Computer Vision Lab., PCVLab, in Columbus, OH until 2010. Thereafter, he was assigned as assistant professor with the Comp. Sci. Dept., Fırat University in 2011. In 2015, he was appointed to Dept. of Air Traffic Management as assistant professor. He is also associated with digital forensics engineering with courtesy. He has been servicing in some of scientific societies' journals and conferences as session chair, referee, program committee, or panelist such as IEEE ITSC, SMCA, IET, TUBITAK, IV, ICCVE, ICPRAM. His research interests include ITS, IV, air traffic, medical data processing, computer vision and image understanding, social computing, ecoinformatics, smart city and mobility. He is the co-founder of Aviation School, Firat University, and co-founder of Ecoinformatics graduate program in the same institution. He is the associate editor of IEEE ITSC in 2018, and ITS Newsletter in 2016, and also he is still in the editorial board of IEEE ITS Podcast.

Affiliations

Mücahit Karaduman[1] · Ahmet Çınar[2] · Haluk Eren[3]

Mücahit Karaduman
mucahit.karaduman@inonu.edu.tr

Ahmet Çinar
acinar@firat.edu.tr

[1] Department of Computer Science, İnönü University, Malatya, Turkey

[2] Engineering Faculty, Computer Engineering, Fırat University, Elazığ, Turkey

[3] The School of Aviation, Air Traffic Management, Fırat University, Elazığ, Turkey